IOP Publishing Journal of Physics B: Atomic, Molecular and Optical Physics
J. Phys. B: At. Mol. Opt. Phys. **49** (2016) 125503 (7pp) doi:10.1088/0953-4075/49/12/125503

Optimal shortcuts for atomic transport in anharmonic traps

Qi Zhang[1], J G Muga[2], D Guéry-Odelin[3] and Xi Chen[1,4]

[1] Department of Physics, Shanghai University, 200444 Shanghai, People's Republic of China
[2] Departamento de Química-Física, UPV-EHU, Apdo 644, E-48080 Bilbao, Spain
[3] Laboratoire Collisions Agrégats Réactivité, CNRS UMR 5589, IRSAMC, Université Paul Sabatier, 118 Route de Narbonne, F-31062 Toulouse CEDEX 4, France
[4] State Key Laboratory of Precision Spectroscopy, East China Normal University, Shanghai 200062, People's Republic of China

E-mail: xchen@shu.edu.cn

Received 15 February 2016, revised 21 April 2016
Accepted for publication 9 May 2016
Published 26 May 2016

Abstract
We design fast trap trajectories to transport cold atoms in anharmonic traps, combining invariant-based inverse engineering, perturbation theory, and optimal control theory. Among the ideal trajectories for harmonic traps, we choose the ones that minimize the anharmonic energy.

Keywords: atom transport, shortcuts to adiabaticity, optimal control theory, anharmonic effect

(Some figures may appear in colour only in the online journal)

1. Introduction

An important goal in current atomic physics is to achieve a thorough control of the motional and internal state of the atom preserving quantum coherence and avoiding undesired excitations. In particular, many experiments and proposals to develop quantum technologies require shuttling cold neutral atoms or ions by moving the confining trap, leaving them at rest and unexcited at the destination site [1–7]. Several approaches to achieve faster than adiabatic transport—shortcuts to adiabaticity—with small (ideally negligible) final excitation but moderate transient motional excitation, have been put forward [8–21]. Reducing the transport time with respect to adiabatic times (long times for which even transient excitations are suppressed) is of interest to achieve faster operations, e.g., in quantum information processing, and also to avoid overheating from fluctuating fields and decoherence. In particular, the combination of invariant-based inverse engineering and optimal control theory, is a versatile toolbox for designing optimal transport protocols, according to different physical criteria or operational constraints [13, 14, 22]. Fast transport can be further optimized with respect to spring-constant errors [20], spring-constant (colored) noise, and position fluctuations [18].

Different transport protocols have been designed for harmonic traps but actual confining traps such as magnetic quadrupole potentials [10], gravitomagnetic potentials [23], Penning-trap potentials [24], and optical dipole traps [25], are anharmonic. The anharmonic terms limit the validity of harmonic approximations and thus the possible process speeds [26]. Their effect has been studied for three-dimensional optical traps [27], perturbatively for condensates [14], and classically in [21]. Reference [15] analyzed as well the coupling between center-of-mass and relative motions of two ions due to anharmonicity. It is known that a force proportional to the acceleration of the trap exactly compensates for the inertial force in the moving trap frame, even for anharmonic potentials, avoiding any excitation [11, 12]. It has been pointed out, however, that this force may be difficult to implement in some systems, such as chains of ions of different mass [12, 15], or due to practical limitations in the strength of the applicable force [15], so that alternative approaches are worth pursuing. A missing piece in the existing studies was an optimal control theory solution, similar to the ones found for expansions of anharmonic traps [28]. The aim of this paper is to fill that gap by finding the transport function that minimizes the anharmonicity. Even if the optimal protocols may be difficult to implement, typically because of discontinuities or jumps in the control parameters,

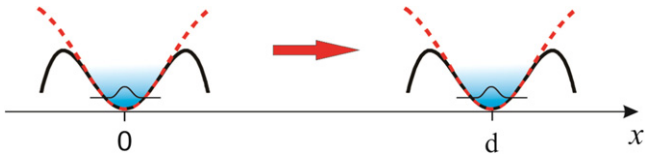

Figure 1. Schematic diagram of atomic transport in an effective one-dimensional Gaussian trap (dashed red line), approximated as a harmonic trap plus anharmonic quartic term (solid black line) from $x = 0$ to $x = d$.

they set a useful reference and bounds that limit what can be achieved with smoother, suboptimal versions.

2. Model, dynamical invariants, and perturbation theory

2.1. Model

We shall consider the following Hamiltonian model for a single particle of mass m moving in one-dimension (with coordinate x) in a moving, anharmonic potential

$$H(t) = \frac{p^2}{2m} + \frac{1}{2}m\omega_0^2[x - x_0(t)]^2 - \eta[x - x_0(t)]^4, \quad (1)$$

where p is the momentum operator and $x_0(t)$ the moving trap center or 'transport function'. As a concrete example, we consider the on-axis potential, $V(x, t) = V_0[1 - \exp(-(x - x_0(t))^2/z_R^2)]$, produced by an optical tweezer made of a focussed Gaussian beam [8, 27]. For $|x - x_0(t)|/z_R \ll 1$, its expansion about its minimum (see figure 1) yields $\omega_0 = (2V_0/mz_R^2)^{1/2}$ and $\eta = V_0/(2z_R^4)$, where V_0 is the depth of the potential, $z_R = \pi w_0^2/\lambda$ is the Rayleigh length, w_0 is the waist of the Gaussian beam, and λ is its wavelength. In the following we choose parameters close to those of the experimental work of [8]: $d = 1 \times 10^{-2}$ m, $\omega_0 = 2\pi \times 20$ Hz, $w_0 = 50\lambda$, $\lambda = 1060$ nm, and $m = 1.44269 \times 10^{-25}$ kg, the mass of ^{87}Rb atoms.

In general, invariant-based engineering of the trap trajectory cannot be applied directly to the Hamiltonian (1), unless it is purely harmonic [12–14] (for $\eta \neq 0$ it does not belong to the family of Lewis–Leach potentials compatible with quadratic-in-momentum invariants [32]). One way out is to add a linear term and thus a compensating force. Some difficulties with this approach mentioned in section 1 will be explained further in section 2.3. A second approximate strategy, which we follow here, is to work out first the family of shortcuts to adiabaticity for a purely harmonic trap, and then combine perturbation theory and optimal control theory to choose the one that minimizes the perturbation, namely, the contribution of the anharmonicity to the time average of the potential energy. In this manner the trap trajectory found for the harmonic trap will in fact be a good solution for the anharmonic one, as it will be confirmed by numerical calculations. To further impose that the anharmonic energy is not a strong perturbation at any instant, the minimization may be carried out under the constraint that the relative displacement between the trap center and the atom remains bounded by some predetermined value.

2.2. Harmonic potential and invariant

We first review briefly the invariant-based inverse engineering approach for (one-dimensional) atomic transport in harmonic traps [12–14]. Harmonic transport is described by the Hamiltonian

$$H_0(t) = \frac{p^2}{2m} + \frac{1}{2}m\omega_0^2[x - x_0(t)]^2. \quad (2)$$

It has the quadratic-in-momentum Lewis–Riesenfeld invariant [31, 32]

$$I(t) = \frac{1}{2m}[p - m\dot{x}_c(t)]^2 + \frac{1}{2}m\omega_0^2[x - x_c(t)]^2, \quad (3)$$

provided $x_c(t)$ satisfies Newton's equation

$$\ddot{x}_c + \omega_0^2(x_c - x_0) = 0, \quad (4)$$

so it may be interpreted as a classical trajectory in the moving harmonic potential. To have $[H_0(t), I(t)] = 0$, at initial time, $t = 0$, and final time, $t = t_f$, so that the Hamiltonian and invariant operators share the same eigensates at the boundary times, as well as $x_0 = x_c$ at the boundary times, we impose

$$x_c(0) = \dot{x}_c(0) = \ddot{x}_c(0) = 0, \quad (5)$$

$$x_c(t_f) = d; \ \dot{x}_c(t_f) = \ddot{x}_c(t_f) = 0, \quad (6)$$

and interpolate $x_c(t)$ in between, for example, by a simple polynomial ansatz

$$x_c(t) = 10\,d(t/t_f)^3 - 15\,d(t/t_f)^4 + 6\,d(t/t_f)^5. \quad (7)$$

The imposed boundary conditions guarantee that there is no final vibrational excitation when the trap is moved from $x_0(0) = 0$ to $x_0(t_f) = d$. The 'transport modes' are solutions of the time-dependent Schrödinger equation given by eigenstates of the dynamical invariant $I(t)$ multiplied by the Lewis–Riesenfeld phase factors, and can be written as [12]

$$\begin{aligned}\langle x|\psi_n(t)\rangle = &\frac{1}{(2^n n!)^{1/2}}\left(\frac{m\omega_0}{\pi\hbar}\right)^{1/4} \\ &\times \exp\left[-\frac{\mathrm{i}}{\hbar}\int_0^t \mathrm{d}t'\left(\lambda_n + \frac{m\dot{x}_c^2}{2} - \frac{m\omega_0^2 x_c^2}{2}\right)\right] \\ &\times \exp\left[-\frac{m\omega_0}{2\hbar}(x - x_c)^2\right]\exp\left(\mathrm{i}\frac{m\dot{x}_c x}{\hbar}\right) \\ &\times H_n\left[\left(\frac{m\omega_0}{\hbar}\right)^{1/2}(x - x_c)\right],\end{aligned} \quad (8)$$

where $\lambda_n = (n + 1/2)\hbar\omega_0$ is real time-independent eigenvalue of the invariant and H_n is a Hermite polynomial. An arbitrary solution of the time-dependent Schrödinger equation $\mathrm{i}\hbar\partial_t\Psi(x, t) = H_0(t)\Psi(x, t)$, can be written as $\Psi(x, t) = \sum_n c_n\psi_n(x, t)$, where $n = 0, 1, \ldots$ and c_n are time-independent coefficients. The instantaneous average energy for a transport mode can be obtained from (2) and (8)

$$\langle\psi_n(t)|H_0(t)|\psi_n(t)\rangle = \hbar\omega_0(n + 1/2) + E_c + E_p, \quad (9)$$

where the first, 'internal' contribution remains constant for each n, $E_c = m\dot{x}_c^2/2$, and $E_p = m\omega_0^2(x_c - x_0)^2/2$ has the form of a potential energy for a classical particle. The instantaneous average potential energy can be written as

$$\langle V(t)\rangle = \frac{\hbar\omega_0}{2}(n + 1/2) + E_p, \tag{10}$$

where here $V = m\omega_0^2(x - x_0)^2/2$.

2.3. Compensating force

Any moving potential $V[x - x_0(t)]$ can in fact be used for excitation-free transport if a linear term $-mx\ddot{x}_0$ is superimposed to compensate for the inertial force [11, 12]. In particular the potential in (1) has to be substituted by

$$V_c = \frac{1}{2}m\omega_0^2(x - x_0)^2 + \eta(x - x_0)^4 - mx\ddot{x}_0, \tag{11}$$

which may be rewritten as

$$V_c = \frac{1}{2}m\widetilde{\omega}_0^2(x - \widetilde{x}_0)^2 + B(x^3, x^4) + C, \tag{12}$$

in which the new time-dependent angular frequency is

$$\widetilde{\omega}_0 = \sqrt{\omega_0^2 + \frac{12}{m}\eta x_0^2}, \tag{13}$$

and the new center of the harmonic part is

$$\widetilde{x}_0 = \frac{\frac{1}{2}m\omega_0^2 x_0 + \frac{1}{2}m\ddot{x}_0 + 2\eta x_0^3}{A}, \tag{14}$$

where $A = m\widetilde{\omega}_0^2/2$, $B = \eta(x^4 - 4x^3x_0)$, and

$$C = \eta x_0^4 + \frac{m}{2}\omega_0^2 x_0^2 - \left(\frac{m}{2}\omega_0^2 x_0 + \frac{m}{2}\ddot{x}_0 + 2\eta x_0^3\right)^2/A \tag{15}$$

is an irrelevant purely time-dependent term. For a purely harmonic trap, $\eta = 0$ and $\widetilde{\omega}_0 = \omega_0$, so the compensating force amounts to shifting the motion of the original trap, see (14). If $\eta \neq 0$, however, the time-dependent potential is not simply a displaced copy of the original one: the harmonic frequency changes with time, and a cubic term appears. Implementing the protocol becomes challenging, as a direct realization of the linear term is limited by experimental constraints, which are more stringent for neutral atoms, for example due to limits on the magnetic field gradient, than for trapped ions [16], where an extra electric field is easy to implement. This motivates an alternative approach that combines inverse engineering with optimal control theory, and treats the anharmonic term as a perturbation.

2.4. Inverse engineering and perturbation theory

In this section the quartic term $V_1 = -\eta[x - x_0(t)]^4$ in (1) is considered as a perturbation. From first-order perturbation theory, the wave function that evolves with (1) may be approximated as

$$|\widetilde{\psi}(t_f)\rangle \simeq |\psi_n(t_f)\rangle - \frac{i}{\hbar}\int_0^{t_f} dt\; U_0(t_f, t)V_1(t)|\psi_n(t)\rangle,$$

where U_0 is the evolution operator for the Hamiltonian (2). We are interested in the time-averaged anharmonic energy

$$\overline{V_1} = \frac{1}{t_f}\int_0^{t_f}\langle\psi_n(t)|V_1(t)|\psi_n(t)\rangle\, dt. \tag{16}$$

Our goal is to minimize it, so that trap trajectories calculated for the harmonic trap remain useful. A lengthy but straightforward calculation gives

$$\overline{V_1} = [6n(n + 1) + 3]\eta\left(\frac{\hbar}{2\,m\omega_0}\right)^2 + \frac{\eta}{t_f}\int_0^{t_f}\left[\left(\frac{\ddot{x}_c}{\omega_0^2}\right)^4 + \frac{3(2n + 1)\hbar}{m\omega_0}\left(\frac{\ddot{x}_c}{\omega_0^2}\right)^2\right]dt. \tag{17}$$

Assuming $\ddot{x}_c = O(d/t_f^2)$ the last term can be neglected for

$$t_f \ll \frac{1}{\omega_0}\sqrt[4]{\frac{md^2\omega_0}{3(2n + 1)\hbar}} \tag{18}$$

(i.e. $t_f \ll 400$ ms for the parameters considered in this paper, see the values below (1), and $n = 0$). Therefore, the time-averaged perturbative energy can be further simplified as

$$\overline{V_1} \simeq [6n(n + 1) + 3]\eta\left(\frac{\hbar}{2\,m\omega_0}\right)^2 + \frac{\eta}{t_f}\int_0^{t_f}\left(\frac{\ddot{x}_c}{\omega_0^2}\right)^4 dt, \tag{19}$$

where the first term is constant, and the second one depends on the classical trajectory x_c. In the following we shall minimize the second term in (19) using OCT. In all examples discussed hereafter $n = 0$.

3. Optimal control theory

Let us define first the 'state' variables and (scalar) control function

$$x_1 = x_c,\;\; x_2 = \dot{x}_c,\;\; u(t) = x_c - x_0, \tag{20}$$

such that (4) gives a system of equation, $\dot{\mathbf{x}} = \mathbf{f}(\mathbf{x}(t), u)$, that is

$$\dot{x}_1 = x_2, \tag{21}$$

$$\dot{x}_2 = -\omega_0^2 u. \tag{22}$$

Our optimal control problem is to minimize the cost function, see (19) and (4)

$$J = \int_0^{t_f} u^4 dt. \tag{23}$$

The boundary conditions (5) and (6) imply that the dynamical system starts at $\{x_1(0) = 0, x_2(0) = 0\}$, and ends up at $\{x_1(t_f) = d, x_2(t_f) = 0\}$, with $u(0) = 0$ and $u(t_f) = 0$. The assumed conditions, $u(t) = 0$ for $t \leqslant 0$ and $t \geqslant t_f$, guarantee that the center of mass and the trap center coincide before and after the transport. At these points jumps of the optimal control will be required to match the boundary conditions. To minimize the cost function (23), we apply Pontryagin's maximal principle [37]. The control Hamiltonian is

$$H_c = -p_0 u^4 + p_1 x_2 - p_2 u, \tag{24}$$

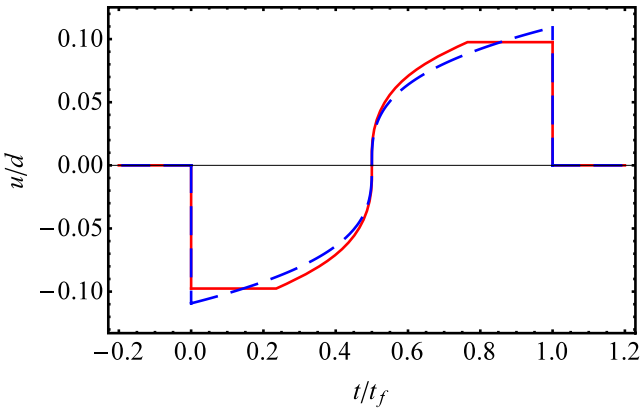

Figure 2. Control function for the optimization with unbounded (dashed blue line) and bounded controls (solid red line) with the bound $\delta = 0.89\delta_U$, where $\delta_U = 14\,d/(3\omega_0^2 t_f^2)$. Parameters: $d = 1 \times 10^{-2}$ m, $\omega_0 = 2\pi \times 20$ Hz, and $t_f = 0.052$ s.

where p_0 is a normalization constant, and p_1, p_2 are Lagrange multipliers. Pontryagin's maximal principle states that for the dynamical system $\dot{\mathbf{x}} = \mathbf{f}(\mathbf{x}(t), u)$, the coordinates of the extremal vector $\mathbf{x}(t)$ and of the corresponding adjoint sate $\mathbf{p}(t)$ formed by Lagrange multipliers fulfill $\dot{\mathbf{x}} = \partial H_c/\partial \mathbf{p}$ and $\dot{\mathbf{p}} = -\partial H_c/\partial \mathbf{x}$, which gives the two costate equations

$$\dot{p}_1 = 0, \tag{25}$$

$$\dot{p}_2 = -p_1, \tag{26}$$

such that for almost all $0 \leqslant t \leqslant t_f$, the values of the control maximize H_c, and $H_c[\mathbf{p}(t), \mathbf{x}(t), u(t)] = c$, with c being a positive constant.

3.1. Unbounded control

According to the maximum principle, the control $u(t)$ maximizes the control Hamiltonian at each time. For simplicity, we choose $p_0 = 1/4$; thus the control Hamiltonian (24) becomes $H_c = -u^4/4 + p_1 x_2 - p_2 u$, so that $\partial H_c/\partial u = 0$ gives $u(t) = (-p_2)^{1/3}$, where u should be real (the branch is chosen to agree with the sign of the radicand). From (25) and (26) we get $p_1 = c_1$, $p_2 = -c_1 t + c_2$ with constants c_1 and c_2. Substituting p_2 into $u(t) = (-p_2)^{1/3}$, and applying the boundary conditions $x_1(0) = 0$, $x_1(t_f) = d$ and $x_2(0) = x_2(t_f) = 0$ in the system of differential equations (21) and (22), we get $c_1 = 5488d^3/27\omega_0^6 t_f^7$ and $c_2 = 2744d^3/27\omega_0^6 t_f^6$, which gives the control function, see figure 2

$$u(t) = \frac{14d}{3\omega_0^2 t_f^2}\left[2\left(\frac{t}{t_f}\right) - 1\right]^{\frac{1}{3}}, \tag{27}$$

and the classical trajectory

$$x_c(t) = \frac{3d}{8}\left[1 - 2\left(\frac{t}{t_f}\right)\right]^{\frac{7}{3}} + \frac{7d}{4}\left(\frac{t}{t_f}\right) - \frac{3d}{8}. \tag{28}$$

The trajectory (28), see figure 3(a), is consistent with the result calculated from the Euler–Lagrange equation, see the appendix. Since the trajectory does not satisfy the boundary conditions $\dot{x}_2(0) = \dot{x}_2(t_f) = 0$, this is a 'quasi-optimal' trajectory.

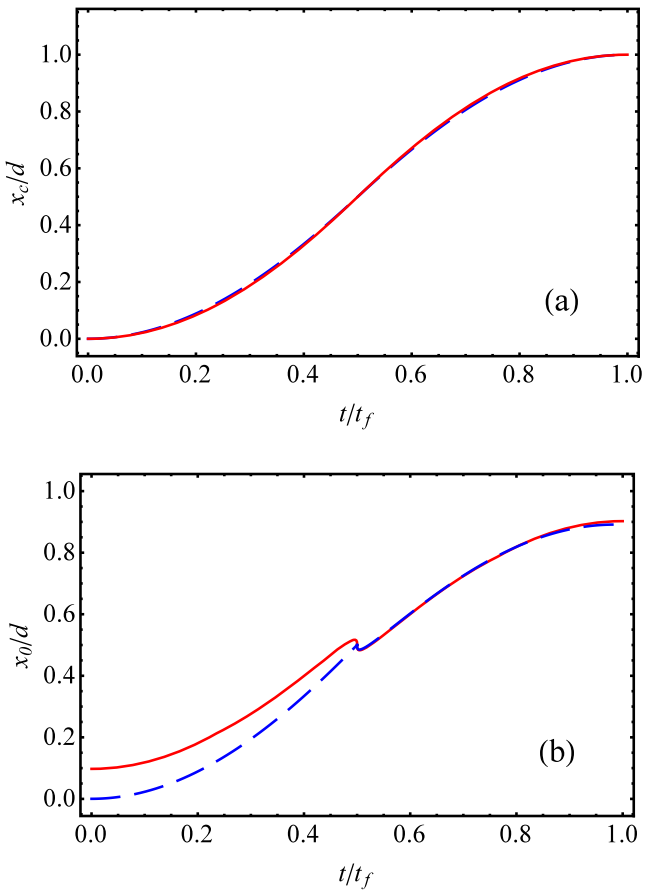

Figure 3. (a) Optimal trajectories of x_c, the center of transport modes, for unbounded (dashed blue line) and bounded controls (solid red line); (b) optimal trajectories of x_0, the trap center, for unbounded (dashed blue line) and bounded controls (solid red line). Same parameters as figure 2.

To guarantee $u(t) = 0$ at $t \leqslant 0$ and $t \geqslant t_f$ and match the boundary conditions, the control function $u(t)$ in unbounded control has to be complemented by the appropriate jumps, see figure 2

$$u(t) = \begin{cases} 0, & t \leqslant 0 \\ \frac{14d}{3\omega_0^2 t_f^2}\left[2\left(\frac{t}{t_f}\right) - 1\right]^{\frac{1}{3}}, & 0 < t < t_f \\ 0, & t \geqslant t_f \end{cases}. \tag{29}$$

From (4), the trap trajectory $x_0(t)$ is thus calculated as $x_0 = x_c - u(t)$, see figure 3(b). Since the control function $u(t)$ in unbounded control is discontinuous, the trap is allowed to change suddenly at $t = 0$ and $t = t_f$.

3.2. Bounded control

Unlike the previous subsection, we may set a bound for the relative displacement between x_c and the trap center, i.e. $|u(t)| \leqslant \delta$ ($\delta > 0$), so that the instantaneous transient energy is never too high. For the bounded control, we set $|u(t)| \leqslant \delta$. Therefore, we assume a symmetrical control function, see

figure 2

$$u(t)=\begin{cases}0, & t\leqslant 0\\ -\delta, & 0<t<t_1\\ -(-c_1t+c_2)^{1/3}, & t_1<t<t_1+t_2,\\ \delta, & t_1+t_2<t<t_{\rm f}\\ 0, & t\geqslant t_{\rm f}\end{cases}\qquad(30)$$

where $t_{\rm f}=2t_1+t_2$ and $c_2=c_1t_{\rm f}/2$. Imposing continuity, the two switching times t_1 and t_2 are given by $t_1=t_{\rm f}/2-\delta^3/c_1$, $t_2=2\delta^3/c_1$. Substituting (30) into (22), we have

$$\dot{x}_{\rm c}(t)=\begin{cases}\omega_0^2\delta t, & 0\leqslant t<t_1\\ -\frac{3}{4}\omega_0^2c_1^{\frac{1}{3}}\left(t-\frac{t_{\rm f}}{2}\right)^{\frac{4}{3}}+c_3, & t_1<t<t_1+t_2,\\ -\omega_0^2\delta(t-t_{\rm f}), & t_1+t_2<t\leqslant t_{\rm f}\end{cases}\qquad(31)$$

which finally gives

$$x_{\rm c}(t)=\begin{cases}\frac{1}{2}\omega_0^2\delta t^2, & 0\leqslant t<t_1\\ -\frac{9\omega_0^2}{28}c_1^{\frac{1}{3}}\left(t-\frac{t_{\rm f}}{2}\right)^{\frac{7}{3}}+c_3t+c_4, & t_1<t<t_1+t_2\\ d-\frac{1}{2}\omega_0^2\delta(t-t_{\rm f})^2, & t_1+t_2<t\leqslant t_{\rm f}.\end{cases}\qquad(32)$$

The continuity of $x_{\rm c}(t)$ and $\dot{x}_{\rm c}$ at $t=t_1$ and $t=t_1+t_2$ determines

$$c_3=\frac{1}{2}\omega_0^2\delta t_{\rm f}-\frac{1}{4c_1}\omega_0^2\delta^4,$$
$$c_4=-\frac{1}{3}\omega_0^2t_{\rm f}^2\delta+\frac{1}{8c_1}\omega_0^2t_{\rm f}\delta^4-\frac{1}{14c_1^2}\omega_0^2\delta^7.$$

The constants c_2, c_3, c_4 and the switching times t_1 and t_2 depend on c_1, which can be found from the continuity of $x_{\rm c}$ at $t=t_1+t_2$,

$$c_1=2\omega_0\sqrt{\frac{\delta^7}{7(\omega_0^2t_{\rm f}^2\delta-4d)}}.\qquad(33)$$

Figure 3 shows the classical and trap trajectories $x_{\rm c}(t)$ and $x_0(t)$. Due to the discontinuity of the control function $u(t)$ at $t=0$ and $t_{\rm f}$, x_0 is discontinuous at the edges, but the classical trajectory $x_{\rm c}(t)$ satisfies the boundary conditions, $x_{\rm c}(0)=0$ and $x_{\rm c}(t_{\rm f})=d$. From (33), the bound should satisfy $\delta\geqslant\delta_L\equiv 4\,d/(\omega_0^2t_{\rm f}^2)$ to make c_1 real. This gives the minimal possible time $t_{\rm f}^{\rm min}=(2/\omega_0)\sqrt{d/\delta}$ for a given bound δ [13]. In addition, for the bound value

$$\delta=\delta_U\equiv\frac{14d}{3\omega_0^2t_{\rm f}^2}\qquad(34)$$

then $t_1=0$, which implies that for δ_U the unbounded control tends to the bounded one. Combining these results, δ is restricted to the interval

$$\delta_U=\frac{14d}{3\omega_0^2t_{\rm f}^2}\geqslant\delta\geqslant\frac{4d}{\omega_0^2t_{\rm f}^2}=\delta_L\qquad(35)$$

for a non-trivial bounded control.

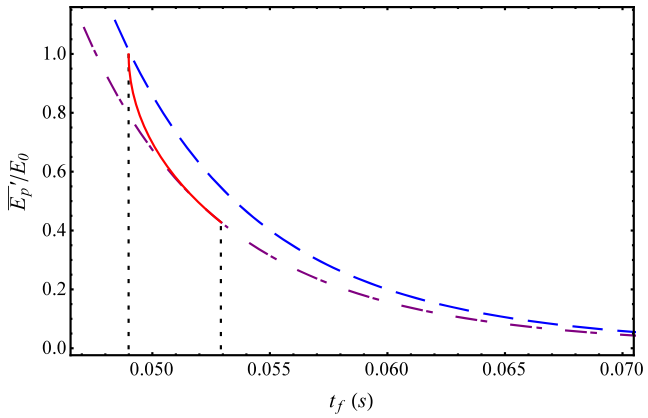

Figure 4. Dependence of time-averaged anharmonic pertubative energy $\overline{E_{\rm p}'}$ (in units of $E_0=\eta\delta^4$) for different protocols, such as optimal trajectories -the ones that minimize the anharmonic energy- with bounded (red solid line) and unbounded (purple dotted–dashed line) controls. The values for the trajectory that minimizes the harmonic potential energy (blue dashed line) are also shown for comparison. The vertical dotted black lines mark the interval $(2/\omega_0)\sqrt{d/\delta}\leqslant t_{\rm f}\leqslant(1/\omega_0)\sqrt{14\,d/3\delta}$. Parameters: $\delta=0.89\delta_U$, $d=1\times10^{-2}$ m, $\omega_0=2\pi\times20$ Hz, $w_0=50\lambda$, $\lambda=1060$ nm, and $m=1.44269\times10^{-25}$ kg the mass of ^{87}Rb atoms. $\delta_U=14\,d/(3\omega_0^2t_{\rm f}^2)$ as in figure 2.

4. Time-averaged anharmonic energy

To analyze the effect of the optimization, we define the time-averaged anharmonic energy as

$$\overline{E_{\rm p}'}\equiv\frac{1}{t_{\rm f}}\int_0^{t_{\rm f}}E_{\rm p}'{\rm d}t=\frac{1}{t_{\rm f}}\int_0^{t_{\rm f}}\eta(x_{\rm c}-x_0)^4{\rm d}t.\qquad(36)$$

Using the optimal trajectory (32) with the bounded control (30), we find, see figure 4

$$\overline{E_{\rm p}'}=\eta\delta^4\left(1-\frac{4\sqrt{7}}{7}\sqrt{1-\frac{4d}{\omega_0^2t_{\rm f}^2\delta}}\right),\qquad(37)$$

which takes the minimal value

$$\overline{E_{\rm p\,min}'}=\frac{392\eta d^4}{9\omega_0^8t_{\rm f}^8},\qquad(38)$$

when $\delta=\delta_L$. This minimal value for anharmonic potential energy is also the value found for optimal unbounded control. When $t_{\rm f}=t_{\rm f}^{\rm min}=(2/\omega_0)\sqrt{d/\delta}$, (37) also gives the maximum value, $E_0=\eta\delta^4$, of anharmonic potential energy with bounded control. The time-averaged anharmonic perturbative energy, $\overline{E_{\rm p}'}$, depends on $t_{\rm f}^{-8}$, to be compared with the time-averaged harmonic energy [12], which is $\propto t_{\rm f}^{-4}$, see below. Figure 4 compares the time-averaged anharmonic energy for bounded and unbounded optimal trajectories.

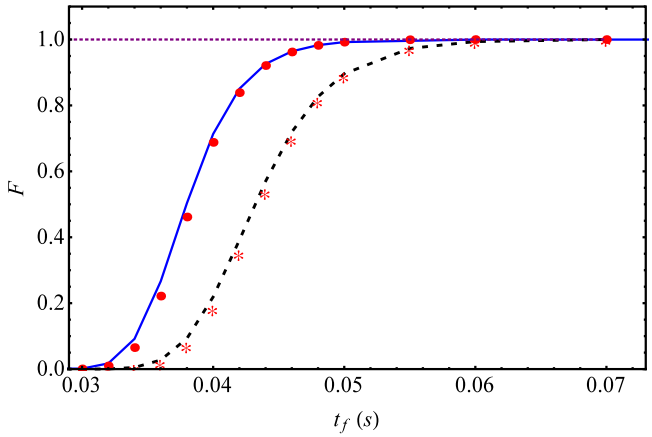

Figure 5. Fidelity with respect to the ground state of the harmonic oscillator of the final state at t_f transported with a Gaussian trap versus t_f for different protocols for the trap center motion, including polynomial ansatz (dashed black line) and 'optimal' solution (blue solid line). The dotted purple line represents the perfect transport for the (unperturbed) harmonic trap for comparison. The fidelities for a trap that includes only quadratic and quartic terms (with '•' and '∗') are indistinguishable from the ones for the Gaussian. Same parameters as figure 4 for unbounded control.

If the perturbative energy, $\overline{E_p'}$, is constrained by some maximally allowed value , t_f should satisfy, see (38),

$$t_f \geqslant \frac{1}{\omega_0}\left(\frac{392\eta d^4}{9\overline{E_p'}}\right)^{1/8}. \tag{39}$$

This is different from the minimal time discussed before $t_f^{\min} = (2/\omega_0)\sqrt{d/\delta}$ [13] as different constraints are imposed.

The time-average of the harmonic energy is

$$\overline{E_p} \equiv \frac{1}{t_f}\int_0^{t_f} E_p dt = \frac{1}{t_f}\int_0^{t_f} \frac{1}{2}m\omega_0^2(x_c - x_0)^2 dt. \tag{40}$$

The 'quasi-optimal' trajectory (28) produces $\overline{E_p} = 96md^2/(15\omega_0^2 t_f^4)$, which is two orders of magnitude larger than the perturbative energy, $\overline{E_p'}$, also for the unbounded control protocol in equation (28) with $t_f = 0.05$ s and the same parameters used above.

Different physical constraints require different optimal trajectories for atomic transport. In particular the classical trajectory $x_c(t) = d(t/t_f)^2(3 - 2t/t_f)$ minimizes the time-averaged (harmonic) potential energy in equation (40) which gives [13] $\overline{E_{p\,\min}} = 6md^2/(\omega_0^2 t_f^4)$. However, the time-averaged anharmonic energy in equation (36) for such trajectory is calculated as $\overline{E_p'} = 1296\eta d^4/(5\omega_0^8 t_f^8)$, which is larger than the minimal value $\overline{E_{p\,\min}'}$ in (38), see figure 4.

Finally, to see the effect of the anharmonic energy minimization on the fidelity of the final state with respect to the one for purely harmonic transport, $F = |\langle\psi_0(t_f)|\tilde{\psi}(t_f)\rangle|$, the final state $\tilde{\psi}(t_f)$ is calculated by solving the time-dependent Schrödinger equation numerically with the split-operator method. Figure 5 shows that the optimal trajectory -for unbounded control- gives a fidelity of nearly one except for very short time. The final state is the ground state after the optimal transport for $t_f \geqslant 0.05$ s. This transport time is the period for the trap, $2\pi/\omega_0 = 0.05$ s, and much shorter than $t_f^{ad} \approx 23.33$ s for adiabatic transport[5]. We have also computed the fidelity for a Gaussian potential with the same harmonic and quadratic terms [30, 38]. This gives results which are indistinguishable from the quartic model.

5. Conclusion

We have found optimal shortcut protocols for fast atomic transport in anharmonic traps. We combine invariant-based inverse engineering, perturbation theory, and optimal control theory to minimize the contribution of the anharmonicity to the potential energy. Numerical calculation of the fidelity demonstrates that the designed optimal trajectory can provide fast and faithful transport in a Gaussian trap. Work is in progress to extend the results to other anharmonic traps like the power-law trap [21] and to transport Bose–Einstein condensates [14].

Acknowledgments

This work was partially supported by the NSFC (11474193), the Shuguang Program (14SG35), the Specialized Research Fund for the Doctoral Program (2013310811003), the Program for Eastern Scholar, the grant NEXT ANR-10-LABX-0037 in the framework of the Programme des Investissements d'Avenir, the Basque Government (Grant IT472-10), MINECO (Grant FIS2015-67161-P), and the program UFI 11/55 of UPV/EHU.

Appendix. Euler–Lagrange equation

Here we use the Euler–Lagrange equation to minimize $\int_0^{t_f}(\dddot{x}_c/\omega_0^2)^4 dt$. We set $\mathcal{L}(t, x_c, \dot{x}_c, \ddot{x}_c) = (\dddot{x}_c/\omega_0^2)^4$, so that the Euler–Lagrange equation

$$\frac{\partial\mathcal{L}}{\partial x_c} - \frac{d}{dt}\left(\frac{\partial\mathcal{L}}{\partial\dot{x}_c}\right) + \frac{d^2}{dt^2}\left(\frac{\partial\mathcal{L}}{\partial\ddot{x}_c}\right) = 0, \tag{A.1}$$

gives

$$\frac{d^2}{dt^2}(\ddot{x}_c)^3 = 0. \tag{A.2}$$

The solution for $x_c(0) = 0$, $x_c(t_f) = d$, and $\dot{x}_c(0) = \dot{x}_c(t_f) = 0$ is

$$x_c(t) = \frac{3d}{8}\left[1 - 2\left(\frac{t}{t_f}\right)\right]^{\frac{7}{3}} + \frac{7d}{4}\left(\frac{t}{t_f}\right) - \frac{3d}{8}. \tag{A.3}$$

[5] The usual adiabaticity criterion becomes $|\dot{x}_0\sqrt{m/(2\hbar\omega_0)}| \ll 1$ for transport in a rigid harmonic trap [13]. Thus adiabatic transport requires $t_f^{ad} \gg d\sqrt{m/(2\hbar\omega_0)}$ for the linear protcol, $x_0(t) = td/t_f$.

References

[1] Hänsel W, Hommelhoff P, Hänsch T W and Reichel J 2001 *Nature* **413** 498
[2] Hänsel W, Reichel J, Hommelhoff P and Hänsch T W 2001 *Phys. Rev. Lett.* **86** 608
[3] Gustavson T L, Chikkatur A P, Leanhardt A E, Görlitz A, Gupta S, Pritchard D E and Ketterle W 2001 *Phys. Rev. Lett.* **88** 020401
[4] Rowe M A *et al* 2002 *Quantum Inf. Comput.* **4** 257
[5] Reichle R, Leibfried D, Blakestad R B, Britton J, Jost J D, Knill E, Langer C, Ozeri R, Seidelin S and Wineland D J 2006 *Fortschr. Phys.* **54** 666
[6] Bowler R, Gaebler J, Lin Y, Tan T R, Hanneke D, Jost J D, Home J P, Leibfried D and Wineland D J 2012 *Phys. Rev. Lett.* **109** 080502
[7] Walther A, Ziesel F, Ruster T, Dawkins S T, Ott K, Hettrich M, Singer K, Schmidt-Kaler F and Poschinger U 2012 *Phys. Rev. Lett.* **109** 080501
[8] Couvert A, Kawalec T, Reinaudi G and Guéry-Odelin D 2008 *Europhys. Lett.* **83** 13001
[9] Murphy M, Jiang L, Khaneja N and Calarco T 2009 *Phys. Rev.* A **79** 020301(R)
[10] Chen D, Zhang H, Xu X, Li T and Wang Y Z 2010 *Appl. Phys. Lett.* **96** 134103
[11] Masuda S and Nakamura K 2010 *Proc. R. Soc.* A **466** 1135
[12] Torrontegui E, Ibanez S, Chen X, Ruschhaupt A, Guéry-Odelin D and Muga J G 2011 *Phys. Rev.* A **83** 013415
[13] Chen X, Torrontegui E, Stefanatos D, Li J S and Muga J G 2011 *Phys. Rev.* A **84** 043415
[14] Torrontegui E, Chen X, Modugno M, Schmidt S, Ruschhaupt A and Muga J G 2012 *New J. Phys.* **14** 013031
[15] Palmero M, Torrontegui E, Guéry-Odelin D and Muga J G 2013 *Phys. Rev.* A **88** 053423
[16] Fürst H A, Goerz M H, Poschinger U G, Murphy M, Montangero S, Calarco T, Schmidt-Kaler F, Singer K and Koch C P 2014 *New J. Phys.* **16** 075007
[17] Deffner S, Jarzynski C and Del Campo A 2014 *Phys. Rev.* X **4** 021013
[18] Lu X J, Muga J G, Chen X, Poschinger U G, Schmidt-Kaler F and Ruschhaupt A 2014 *Phys. Rev.* A **89** 063414
[19] Palmero M, Bowler R, Gaebler J P, Leibfried D and Muga J G 2014 *Phys. Rev.* A **90** 053408
[20] Guéry-Odelin D and Muga J G 2014 *Phys. Rev.* A **90** 063425
[21] Zhang Q, Chen X and Guéry-Odelin D 2015 *Phys. Rev.* A **92** 043410
[22] Stefanatos D, Ruths J and Li J S 2010 *Phys. Rev.* A **82** 063422
[23] Bertoldi A and Ricci L 2010 *Phys. Rev.* A **81** 063415
[24] Alonso J, Leupold F M, Keitch B C and Home J P 2013 *New J. Phys.* **15** 023001
[25] Ahmadi P, Behinaein G, Timmons B P and Summy G S 2006 *J. Phys. B: At. Mol. Opt. Phys.* **39** 1159
[26] Chen X and Muga J G 2010 *Phys. Rev.* A **82** 053403
[27] Torrontegui E, Chen X, Modugno M, Ruschhaupt A, Guéry-Odelin D and Muga J G 2012 *Phys. Rev.* A **85** 033605
[28] Lu X J, Chen X, Alonso J and Muga J G 2014 *Phys. Rev.* A **89** 023627
[29] Léonard J, Lee M, Morales A, Karg T M, Esslinger T and Donner T 2014 *New J. Phys.* **16** 093028
[30] Kinoshita T, Wenger T and Weiss D S 2004 *Science* **305** 1125
[31] Lewis H R and Riesenfeld W B 1969 *J. Math. Phys.* **10** 1458
[32] Lewis H R and Leach P G 1982 *J. Math. Phys.* **23** 2371
[33] Chen X, Ruschhaupt A, Schmidt S, Del Campo A, Guéry-Odelin D and Muga J G 2010 *Phys. Rev. Lett.* **104** 063002
[34] Ibáñez S, Chen X, Torrontegui E, Muga J G and Ruschhaupt A 2012 *Phys. Rev. Lett.* **109** 100403
[35] Berry M V 2009 *J. Phys. A: Math. Theor.* **42** 365303
[36] Chen X, Torrontegui E and Muga J G 2011 *Phys. Rev.* A **83** 062116
[37] Pontryagin L S *et al* 1962 *The Mathematical Theory of Optimal Processes* (New York: Interscience Publishers)
[38] Saleh B E A and Teich M C 2007 *Fundamentals of Photonics* 2nd edn (New York: Wiley)